Journal of Integrative Agriculture 2016, 15(2): 475–491

Available online at www.sciencedirect.com

ScienceDirect

REVIEW

Estimating the crop leaf area index using hyperspectral remote sensing

LIU Ke[1, 2], ZHOU Qing-bo[1, 2], WU Wen-bin[1, 2, 3], XIA Tian[3], TANG Hua-jun[1, 2]

[1] *Key Laboratory of Agri-Informatics, Ministry of Agriculture, Beijing 100081, P.R.China*
[2] *Institute of Agricultural Resources and Regional Planning, Chinese Academy of Agricultural Sciences, Beijing 100081, P.R.China*
[3] *College of Urban & Environmental Sciences, Central China Normal University, Wuhan 430079, P.R.China*

Abstract

The leaf area index (LAI) is an important vegetation parameter, which is used widely in many applications. Remote sensing techniques are known to be effective but inexpensive methods for estimating the LAI of crop canopies. During the last two decades, hyperspectral remote sensing has been employed increasingly for crop LAI estimation, which requires unique technical procedures compared with conventional multispectral data, such as denoising and dimension reduction. Thus, we provide a comprehensive and intensive overview of crop LAI estimation based on hyperspectral remote sensing techniques. First, we compare hyperspectral data and multispectral data by highlighting their potential and limitations in LAI estimation. Second, we categorize the approaches used for crop LAI estimation based on hyperspectral data into three types: approaches based on statistical models, physical models (i.e., canopy reflectance models), and hybrid inversions. We summarize and evaluate the theoretical basis and different methods employed by these approaches (e.g., the characteristic parameters of LAI, regression methods for constructing statistical predictive models, commonly applied physical models, and inversion strategies for physical models). Thus, numerous models and inversion strategies are organized in a clear conceptual framework. Moreover, we highlight the technical difficulties that may hinder crop LAI estimation, such as the "curse of dimensionality" and the ill-posed problem. Finally, we discuss the prospects for future research based on the previous studies described in this review.

Keywords: hyperspectral, inversion, leaf area index, LAI, retrieval

1. Introduction

The leaf area index (LAI) is usually defined as the one-sided area of leaves per unit ground area (Chen and Black 1992). The LAI reflects the biochemical and physiological processes of vegetation, thereby indicating the productivity of vegetation, and it serves as an input variable in land surface process models. Therefore, understanding the LAI of a crop and its dynamics is very important for a wide range of agricultural studies, such as crop growth monitoring and crop yield estimation (Fang *et al.* 2011).

Received 27 November, 2014 Accepted 6 April, 2015
LIU Ke, Tel: +86-17780637083, E-mail: billc_st@163.com; Correspondence ZHOU Qing-bo, Tel: +86-10-82106237, E-mail: zhouqingbo@caas.cn; TANG Hua-jun, Tel: +86-10-82105070, E-mail: tanghuajun@caas.cn

doi: 10.1016/S2095-3119(15)61073-5

Remote sensing techniques are known to have unique advantages for obtaining multitemporal, spatially continuous crop LAI data over a large area. In most cases of LAI estimation using remote sensing, the leaves are assumed to be homogeneously distributed. The LAI values estimated under this assumption are referred to as the effective LAI (LAI_{eff}) (Chen and Black 1992). LAI_{eff} has the same main functions as the true LAI. The LAI_{eff} and true LAI can be interconverted *via* a clumping index (Chen *et al.* 2005). Conventional multispectral (also referred to as broadband) remote sensing, which divides a discontinuous spectral coverage into several broad bands, has been used frequently for obtaining LAI over time and space (Chen and Cihlar 1996; Cohen *et al.* 2003; Fang and Liang 2005; Durbha *et al.* 2007). More recently, hyperspectral remote sensing has attracted increasing attention for LAI estimation because it provides continuous spectral coverage and achieves a spectral resolution of $10^{-2}\lambda$ (where λ is the wavelength), i.e., the spectral resolution is <10 nm in the range of 400–2 500 nm (Jensen 2009). Three types of hyperspectral remotely sensed data can be identified according to the platform used: nonimaging or imaging *in situ* easurements, airborne images and spaceborne images. However, because of the nonlinearity of the methods employed for LAI estimation and spatial heterogeneity, the LAI values obtained vary according to the spatial resolution, i.e., scaling effects, which should be considered when comparing or integrating LAIs estimated using data acquired at various resolutions or with different types of sensors (Garrigues *et al.* 2006).

In general, the approaches employed for crop LAI estimation using hyperspectral data can be categorized into three types according to the methods utilized: approaches based on statistical models, approaches based on physical models (i.e., canopy reflectance models), and hybrid inversions. Approaches based on statistical models first compute characteristic parameters (also referred to as “estimators”) that are significantly correlated with the LAI. Next, a statistical predictive model of the LAI is constructed based on the relationships between the characteristic parameters and the known LAI values in sample plots using statistical approaches. Canopy reflectance models simulate the reflectance of the canopy using vegetation parameters as inputs. The LAI can be estimated by computing a physical model in reverse using spectral reflectance as the input and vegetation variables, including LAI, as the output; i.e., physical model inversion. Hybrid inversion approaches involve the integrated application of statistical and physical models to exploit their respective advantages. Crop LAI retrieval using hyperspectral data has potential problems, such as the low signal-to-noise ratios (SNRs) of some hyperspectral data, the “curse of dimensionality” (see section 2.2), problems of saturation (see section 3.1) and the ill-posed problem when inverting physical models (see section 4.3). In addition, more sophisticated methods for LAI retrieval that maximize the potential utilization of hyperspectral data merit further study (see sections 2.1 and 6.2).

Motivated by the increasingly widespread application of hyperspectral data in LAI estimation and the development of relevant approaches, this review aims to provide an overview of crop LAI estimation using hyperspectral data. First, we compare hyperspectral data with multispectral data in section 2. Second, crop LAI estimation based on statistical models and physical models are reviewed separately in sections 3 and 4, and compared in section 6.1. Finally, a conceptual framework for LAI estimation is presented in section 6.2, and the prospects for future research are discussed.

2. Advantages and limitations of hyperspectral data for crop LAI estimation

2.1. Advantages of hyperspectral data for retrieving LAI

Theoretically, the superior spectral resolution of hyperspectral data should yield spectral details that are obscured in multispectral data (Schlerf *et al.* 2005). However, the advantages of hyperspectral data compared with multispectral data for LAI estimation remain controversial. First, hyperspectral data facilitate waveform analysis techniques such as LAI retrieval using red-edge parameters (Herrmann *et al.* 2011). Hyperspectral data also improve the performance of conventional LAI estimators; e.g., spectral reflectance (Lee *et al.* 2004), the second principle component (Pu and Gong 2004), and the first or second spectral derivative (Fan *et al.* 2010a). Many studies have shown that hyperspectral data can improve the accuracy of LAI estimation (Lee *et al.* 2004; Pu *et al.* 2008; Fan *et al.* 2010b; Verrelst *et al.* 2012; Duan *et al.* 2014). However, opposing views also exist (Spanner *et al.* 1994; Jacquemoud *et al.* 1995; Li *et al.* 1997; Broge and Leblanc 2000). For instance, Li *et al.* (1997) proposed that structural parameters are independent of the spectrum; therefore, increasing the number of bands cannot provide more information about these parameters. However, this conclusion is based only on a sensitivity analysis of the parameters used in canopy reflectance models, without considering the effects of the factors in the actual LAI retrieval procedures, such as nuances in the sensitivity of LAI among hyperspectral bands, and the bias between simulated and remotely sensed canopy reflectance. Moreover, some comparative studies themselves are imperfect (Lee *et al.* 2004), such as those performed using early-generation, low SNR airborne visible/infrared imaging spectrometer (AVIRIS) data (Spanner *et al.* 1994) and those that relied excessively on physical model simulations rather than *in situ* measurements (Jacquemoud *et al.* 1995; Broge and

Leblanc 2000). In addition, most of these comparative studies (Spanner *et al.* 1994; Broge and Leblanc 2000; Lee *et al.* 2004; Schlerf *et al.* 2005) relied on vegetation indices (VIs) rather than more innovative estimators of LAI (such as red-edge parameters) or innovative approaches for retrieving LAI (such as by inverting physical models), which may utilize hyperspectral data more efficiently. In conclusion, more sophisticated and comprehensive studies are needed in the future to clarify whether, and possibility why, hyperspectral data improve LAI estimations.

The accuracy of LAI estimation is affected by a complex array of external factors (atmospheric scattering, soil background reflectance, and the effects of mixed pixels) and other parameters in physical models (such as the chlorophyll content and average leaf angle), i.e., the "ill-posed problem" (see section 4.3). Hyperspectral data have been reported helpful for end-member extraction of mixed pixels (Franke *et al.* 2009), atmospheric correction (Gao *et al.* 2009; Perkins *et al.* 2012), and improving the estimation accuracy of some insensitive variables, e.g., chlorophyll content and average leaf angle (Atzberger and Richter 2012). Therefore, even if hyperspectral data provide no direct and significant improvements when retrieving LAI, as stated by Li *et al.* (1997), these data have greater potential for reducing the uncertainties that affect LAI retrieval, thereby improving the accuracy and stability of the resulting LAI indirectly as a consequence. To achieve this objective, the current techniques used for LAI retrieval need to be improved dramatically to fit hyperspectral data; i.e., estimators of LAI and procedures of band selection should be designed for hyperspectral data; the LAI estimation should eventually benefit from the enhancement in estimating other variables. See section 6.2 for further discussion.

2.2. Limitations of hyperspectral data for crop LAI estimation

In previous studies, the most important problems related to hyperspectral data included low SNRs and high correlations between bands.

The quality of hyperspectral data varies depending on the sensors, the bands and the directions of observations. Some of the bands obtained using HyMap (Schlerf *et al.* 2005), UAV-HYPER (Duan *et al.* 2014), and DAIS-7915 (Ben-Dor *et al.* 2002) sensors have low SNRs. Therefore, bands with low radiometric quality should be eliminated from further analysis. Some images have a mask layer that indicates the image quality; e.g., compact high-resolution imaging spectrometer/project for on-board autonomy (CHRIS/PROBA) (Li *et al.* 2011). Alternatively, we must compute the SNR manually; e.g., Gao (1993) proposed a possible algorithm based on the local means and local standard deviations in small imaging blocks. In addition, random noise can also be eliminated using filtering approaches, as demonstrated by Othman and Qian (2006) and Fan *et al.* (2010b).

Hyperspectral data comprise of numerous highly correlated bands, but the multicollinearity between there bands and random errors in spectral measurements lead to the so-called "curse of dimensionality", which has the following implications. First, statistical predictive models constructed using highly correlated samples have a high coefficient of determination but poor predictive capabilities (Lee *et al.* 2004). Second, bands that are insensitive to LAI require additional computational time, but they distort the accuracy of LAI retrieval. Therefore, it is necessary to reduce the dimensionality of hyperspectral data (Jensen 2009), which can be achieved either by computing the characteristic parameters of LAI (see section 3.1) or by selecting relatively uncorrelated bands that contain the main information in the original data. The former approach is used mainly in statistical predictive model of LAI, the latter method is used mainly for LAI estimation by inverting physical models. The band selection process comprises two steps: selecting relatively uncorrelated bands and selecting bands that are sensitive to the parameters of interest; i.e., LAI. Stepwise regression (Lee *et al.* 2004; Huang *et al.* 2011a) was shown to be feasible for identifying multicollinearity. Sensitivity and uncertainty analysis approaches can be used to select sensitive hyperspectral bands of LAI. Among them, uncertainty and sensitivity matrix (USM) (Li *et al.* 1997, 2001) and extended fourier amplitude sensitivity test (EFAST) (Saltelli *et al.* 1999), correlation analysis and principal components analysis (Huang *et al.* 2011a) are particularly recommended. The optimum hyperspectral bands for LAI estimation are still debated, no commonly accepted principle can be proposed. Some studies suggest estimating a variable using the band which is the most sensitive to it. Thus, the selected bands for LAI retrieval are mainly within red-NIR (near infrared) range (Li *et al.* 1997; Zhu *et al.* 2011). Some other studies selected bands covering red-NIR-SWIR (short wave infrared) spectra (Lee *et al.* 2004; Huang *et al.* 2011a, b). Eklundh *et al.* (2001), Cohen *et al.* (2003), and Lee *et al.* (2004) proposed the importance of SWIR for LAI estimation. Generally speaking, uncorrelated and the most sensitive bands in Red-NIR-SWIR range were selected for retrieving LAI. There are also studies that ignore band selection and use all hyperspectral bands (Duan *et al.* 2014).

It should be noted that in some applications, the capacity for rapid and dynamic crop monitoring on a large scale is usually the most preferred advantage of remote sensing techniques (Yang *et al.* 2007a; Wu *et al.* 2008, 2010). In this case, multispectral data are thought sufficient only if the accuracy obtained satisfies a specific tolerance. By con-

trast, an excessive focus on accuracy usually complicates the algorithm and sacrifices the computational efficiency. Moreover, the revisit period and image coverage of hyperspectral data sources (e.g., hyperion and CHRIS/PROBA) are not better than those of multispectral sources (e.g., moderate resolution imaging spectroradiometer (MODIS) and operational land imager (OLI) onboard the Landsat 8 satellite). Therefore, in applications, it is necessary to perform a comprehensive examination of the scope of the study, the desired accuracy and temporal resolution to determine a suitable spectral resolution.

In conclusion, hyperspectral data are considered to be promising for LAI retrieval, although they may have potential low SNR and they are affected by the curse of dimensionality. Future studies may explore methods for LAI estimation using hyperspectral data. In applications, the requirements of the study should be considered to determine the most appropriate data sources.

3. Crop LAI estimation based on statistical models

In LAI estimation based on statistical models, the characteristic parameters (also referred to as "estimators") that have significant correlations with the LAI are computed firstly from the canopy spectrum. Next, the statistical relationships are constructed between the characteristic parameters and the known LAI values in sample plots. This statistical predictive model is then used to compute the LAI values throughout the whole image.

3.1. Characteristic parameters for estimating crop LAI

The flowing types of characteristic parameters are commonly applied for LAI estimation. First, VIs are designed to depict distinctive spectral characteristics of vegetation, e.g., high reflectance in near inferred bands and absorption in red bands, with a one-dimensional index. Hyperspectral vegetation indices were developed for hyperspectral data. Some of them are conventional VIs computed with narrow band reflectance (Schlerf *et al.* 2005), whereas others are newly constructed using waveform analysis techniques (Broge and Leblanc 2000). Different VIs have specific sensitivities and resistances to different factors or disturbances, but they are all affected by the problem of saturation; i.e., VIs are generally insensitive to the LAI when the LAI is greater than 3–6 because VI-LAI correlations are not linear or stable, especially under various influences (Haboudane 2004). Moreover, VIs resist disturbances from the soil and atmosphere, but only in a rather limited level (Broge and Leblanc 2000). Second, variables that describe the characteristic spectra of vegetation are also used for LAI estimation, for instance: red-well position, red-edge inflection position (Pu *et al.* 2003), area of red-edge peak, NIR-platform position, red-edge amplitude (Filella and Penuelas 1994) and NIR-platform amplitude (Zhao *et al.* 2002). They have been reported to be better estimators compared with VIs (Herrmann 2011). Third, many studies have used spectral reflectance and spectral derivatives. Hyperspectral reflectance was also reported to be a better estimator of LAI compared with VIs in terms of sensitivity and stability (Xia *et al.* 2013). However, hyperspectral reflectance is affected by the curse of dimensionality (see section 2.2), and it is more vulnerable to atmospheric scattering and background reflectance. Thus, the first or second derivative of the spectrum has been used to remove background and atmospheric disturbance, thereby enhancing subtle variations in the spectral reflectance (Johnson and Billow 1996; Fan *et al.* 2010b). However, spectral derivatives enhance high-frequency random noise, which means that certain types of noise reduction processing are necessary (Fan *et al.* 2010b). Finally, some features derived from principal components analysis (PCA) and wavelet transform (WT) are also used widely. PCA and WT are mathematical procedures for data compression, which can convert highly related spectral reflectance data into several uncorrelated "features" to avoid the curse of dimensionality. Pu and Gong (2004) proposed that energy features derived from WT are the most effective for LAI estimation, followed by principal components and spectral reflectance. Besides, PCA and WT effectively reduce the dimension of hyperspectral reflectance and therefore avoid the curse of dimensionality. However, PCA and WT do not enhance the spectral characteristics of the data (Johnson and Billow 1996; Fan *et al.* 2010b).

3.2. Construction of statistical models

Once the characteristic parameters of the LAI are computed, their relationships with known LAI values are determined using statistical approaches to construct statistical predictive models of the LAI.

Exponential or linear regression, artificial neural networks (abbr. neural networks, NNs), support vector regression (SVR), and partial least squares (PLS) have been used to construct statistical predictive model of LAI (Table 1). In particular, conventional exponential and linear regression are usually applied to the low-dimensional characteristic parameters of LAI, such as VIs and red-edge variables, whereas NN, SVR, and PLS are applied to high-dimensional characteristic parameters, i.e., spectral reflectance and spectral derivatives. NNs are considered to be an incomparable approach with excellent accuracy and efficiency when fitting complex, high-dimensional, nonlinear relationships, e.g., the relationships between

Table 1 Technical specifications of representative leaf area index (LAI) estimation studies based on statistical models

Recommended characteristic parameter[1)]	Statistic approach[2)]	Data source	Reference
Reflectance	CCA	AVIRIS, ETM+	Lee *et al.* (2004)
Reflectance	NN	MERIS	Bacour *et al.* (2006)
Reflectance	NN	Measurement	Xia *et al.* (2013)
MTVI2, MCARI2	Linear	CASI	Haboudane (2004)
PVI	Linear	HyMap	Schlerf *et al.* (2005)
Red-edge amplitude, Area of the red-edge peak	Exponential	Measurement	Filella and Penuelas (1994)
DVI	Exponential, linear	TM	Yang *et al.* (2007b)
REP, RWP	Exponential	Hyperion	Pu *et al.* (2003)
REP, NDVI	Linear exponential	VENμS, Sentinel-2	Herrmann *et al.* (2011)
Reflectance	PLS	Measurement	
SAVI2	Exponential	Synthetic	Broge and Leblanc (2000)
Reflectance	Polynomial	SPOT	Houborg and Boegh (2008)
SR	Linear	TM	Eklundh *et al.* (2003)
WT	Linear		Dongmei *et al.* (2010)
Multiple VIs	CCA	ETM+	Cohen *et al.* (2003)
NDVI	Linear	*In situ* measurement RapidEye	Tillack *et al.* (2014)
Reflectance	SVR	*In situ* measurement	Yang *et al.* (2011)
Reflectance, VIs	NN, exponential	Synthetic	Baret *et al.* (1995)
PCA, VIs	Linear, exponential	FY3	Feng *et al.* (2013)

[1)] MTVI2, a modified triangular vegetation index; MCARI2, a modified chlorophyll absorption ratio index; PVI, perpendicular vegetation index; DVI, difference vegetation index; REP, red-edge position; RWP, red-well position; NDVI, normalized difference vegetation index; SAVI2, the second soil-adjusted vegetation index; SR, simple ratio; WT, wavelet transformation; VIs, vegetation indices; PCA, principal components analysis.

[2)] CCA, canonical correlation analysis; NN, artificial neural network; Linear, linear regression; Exponential, exponential regression; PLS, partial least squares; Polynomial, polynomial regression; SVR, support vector regression.

LAI and hyperspectral reflectance, (Baret *et al.* 1995; Huang *et al.* 2011b). PLS analysis is another alternative for handling both high- and low-dimensional estimators. Indeed, PLS can handle multicollinearity and random noise, which makes it particularly suitable for the hyperspectral spectrum (Herrmann *et al.* 2011). Moreover, the support vector machine (SVM) is a supervised nonparametric statistical learning approach, which is known to be reliable for regression, especially with high-dimensional inputs (Durbha *et al.* 2007). Based on SVM, SVR provides excellent generalization capabilities with good computational efficiency, and it requires fewer samples than NNs (Durbha *et al.* 2007). Although SVR is not used widely for LAI estimation, it is promising in theory for both high- and low-dimensional estimators, and thus it should be tested in future study (Yang *et al.* 2011). Conventional regression methods are inadequate when using multiple estimators, such as multitemporal data or multiple VIs together. Thus, canonical correlation analysis is applied to integrate multiple estimators into a single index (Cohen *et al.* 2003; Lee *et al.* 2004).

In summary, there is generally no perfect characteristic parameter, even for a specific type of vegetation or data source. Thus, researchers must make their selections based on the following considerations: the sensitivity of an estimator to the LAI within the expected range (Gonsamo and Pellikka 2012), the feasibility of computing a specific estimator, disturbances due to the atmosphere and soil background and random noise in the remote sensing data. Conventional regression methods are suitable for low-dimensional estimators, whereas NNs, PLS, and SVR can handle high-dimensional nonlinear relationships (Table 1). Nevertheless, according to previous studies, no optimal regression technique has been proposed, even for a specific estimator. In some studies, several regression techniques are tested to find the best fit (Eklundh *et al.* 2003; Yang *et al.* 2007b).

4. Crop LAI estimation based on physical models

Physical models (i.e., canopy reflectance models) simulate the bidirectional reflectance and transmittance of canopies using canopy variables (e.g., LAI and leaf angle distribution), variables that describe the observation geometry (e.g., zenith and azimuth angle of sunlight and the observation direction), and the spectra of individual leaves and the soil background as model inputs. In particular, the LAI is the most sensitive variable in the NIR and red wavelength (Li *et al.* 1997; Xiao *et al.* 2013), so the LAI is retrieved mainly based on reflectance in NIR and red. In practice, the spectral signatures of leaves and soil can be simulated further using leaf or soil reflectance models with leaf biochemical parameters (e.g., leaf chlorophyll/water content) or soil variables as the inputs. Such coupling makes it feasible to estimate the parameters of leaves and soil directly from remotely sensed data. For example, the PROSPECT model coupled with the

SAIL (scattering by arbitrarily inclined leaves) model, i.e., the PROSAIL model, has been applied widely for retrieving the chlorophyll content, water depth, fAPAR, etc. (Jacquemoud *et al.* 2009). Theoretically, the canopy/leaf variables (including LAI) can be determined by inverting physical models using remotely sensed canopy spectra as inputs. However, because of the complexity of physical models, approaches that obtain numerical solutions (referred to as inversion strategies) to the models are necessary for LAI estimation (see section 4.2). In this review, we collected representative studies that applied physical models for LAI estimation by searching Google Scholar[TM] using the key words "leaf area index" and the names of relevant models. The relevant studies in the first 10 pages, which have been sorted by relevance, are categorized and plotted in Fig. 1.

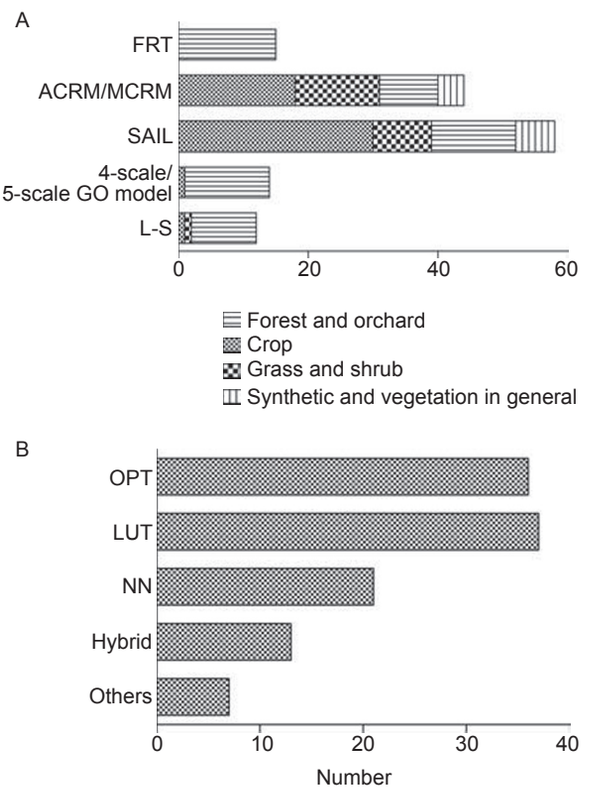

Fig. 1 Number of publications describing leaf area index (LAI) estimation by inverting physical models. A, sorted by the physical models applied. B, sorted by the inversion approaches of physical models. FRT, Kuusk-Nilson forest reflectance model; ACRM, a two-layer canopy reflectance model; MCRM, Markov chain reflectance model; SAIL, scattering by arbitrarily inclined leaves; GO, geometric optical; L-S, Li-Strahler model; OPT, iterative optimization; LUT, lookup table; NN, neural network. The same as below.

4.1. Major reflectance models

In general, four categories of reflectance models can be distinguished (Schlerf and Atzberger 2006): radiative transfer (RT) models, geometric optical (GO) models, RT/GO hybrid models, and computer simulation models.

RT models, which are also known as analytical or turbid models, simulate the interaction between incident radiation and a homogeneous medium. Thus, in canopy RT models, the canopy is assumed to be continuous with horizontally homogeneous layers of evenly distributed leaves with a given geometry and density (Fig. 2-A).

The intensively studied SAIL model (Verhoef 1984) (including the SAIL including hot spot effect (SALH)) model, Fig. 3-A) and a series of models developed from the Nilson-Kuusk (N-K) model (except the FRT model, Fig. 3-B) are representative examples of canopy RT models. SAIL approximates the radiation inside a canopy based on four fluxes: diffuse irradiance in the direction of observation E_0, upward and downward diffuse flux E^+, E^- and the direct solar flux E_s. Four differential equations have been proposed, which are controlled by nine extinction and backscattering coefficients. The extinction and backscattering coefficients can be further expressed using canopy variables and observation geometry. The N-K model (Nilson and Kuusk 1989) improved the bidirectional gap probability algorithm proposed originally by Ross (1981) to express bidirectional reflectance and hotspot effect. The N-K model computes scattered radiance as the sum of three components: $\rho=\rho_c^1+\rho_s^1+\rho^{MULT}$

Where, ρ_c^1 and ρ_s^1 are the first-order reflectance from the canopy and soil respectively, and ρ^{MULT} is the multiple

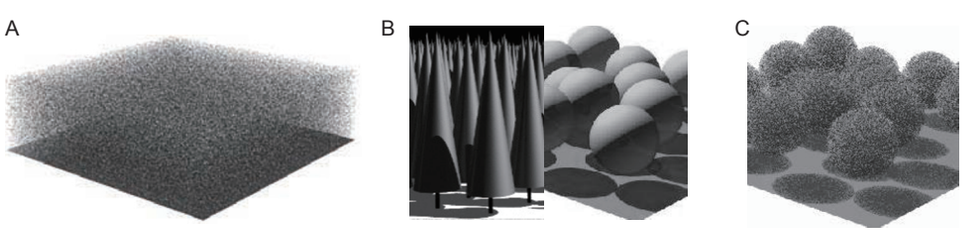

Fig. 2 The scenarios assumed by canopy reflectance models (Widlowski *et al.* 2007). GO, geometric optical; RT, radiative transfer. The same as below.

scattering on the foliage and soil elements.

A series of canopy RT models have been developed from the N-K model (Fig. 3-B). For example, to obtain more realistic simulation of radiative transformation in canopies with a strong vertical structure, such as corn, Kuusk (1995b) improved the expression of leaf angle distribution function (G function) using Markov chain theory:

$$G_{eff}(\theta)=\left\{\left[1-(1-\lambda_z)\frac{1-\exp(-Y(\theta))}{Y(\theta)}\right]\right\}G(\theta)$$

Where, λ_z is the Markov coefficient; $Y(\theta)$=arctan(θ); and $G(\theta)$ is the original G function.

At present, the SAIL and ACRM (a two-layer canopy reflectance model) are relevantly mature and accurate RT models for continuous canopies and thus they are used most widely (Fig. 1-A).

Based on a much more realistic scenario, the conventional RT models were developed into three-dimensional (3-D) RT models. For example, the discrete anisotropic radiative transfer (DART) model (Gastellu-Etchegorry *et al.* 2004) simplifies the actual landscape into rectangular cells that comprise a specific turbid medium (e.g., canopy, water, or atmosphere) and plane opaque surface (e.g., soil and the roofs of building). Thus, it can represent various aspects of urban and natural landscape, as well as the effects of topography and atmosphere. 3-D RT models provide more realistic scenes, which are free from the errors caused by simplifying the process of radiative transformation. Thus, they can provide more accurate representations of the actual (complex) canopy. They have been applied increasingly in recent years because of developments in the capacity of computers and inversion strategies, e.g., the DART model (Darvishzadeh *et al.* 2008; Hernández-Clemente *et al.* 2014) and forest light interaction model (FLIGHT) (Guillen-Climent *et al.* 2012). Although they are not used widely for crop LAI estimation, they may be promising for future studies, especially in complex conditions, e.g., row crops or heterogeneous canopies in the early stages of crop growth.

The hypothesis of a homogeneous and continuous canopy in RT models is unrealistic, and it may lead to errors, especially with discrete vegetation, e.g., forest and wheat before elongation. Thus, GO models, hybrid models, and 3-D computer simulation models were developed. Typical GO models such as the Li-Strahler model (Li and Strahler 1986) assume that individual canopies are opaque geometric shapes (e.g., corn or ellipsoid), which cast shadows on the soil background (Fig. 2-B), where the reflected radiance is the area-weighted sum of the radiance from the illumi-

A

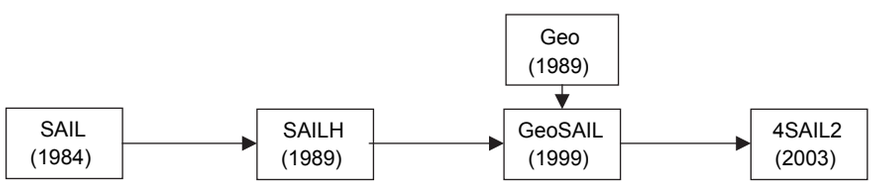

Type	Turbid	Turbid	Hybrid (3-D)	Hybrid (3-D)
Description	Calculating extinction coefficients based on an arbitrary (i.e., real) leaf inclination angle, rather than projecting leaves onto three orthogonal planes	Considering the hotspot effect	Combination of the Geo (GO) model with SAIL for discrete canopies; two layers of canopy	Non-Lambertian soil reflectance model; the additional consideration of vegetation with ground or crown coverage <1; considering clumping effects
Reference	Verhoef (1984)	Kuusk (1991)	Huemmrich (2001)	Verhoef and Bach (2003)

B

Type	Turbid	Turbid	Turbid	Turbid
Description	See section 4.1	Expression of first-order scattering based on the N-K model and expression of multiple scattering based on the SAIL model	New G function based on Markov chain theory for canopies with vertical structure	Considering the reflectance of understory vegetation
Reference	Nilson and Kuusk (1989)	Kuusk (1994, 1995a)	Kuusk (1995b)	Kuusk (2001)

Fig. 3 The evolution of RT models. A, representative versions of scattering by arbitrarily inclined leaves (SAIL) model. B, series of canopy reflectance models developed from the N-K model. N-K, Nilson-Kuusk model; MSRM, multispectral canopy reflectance model; ACRM, a two-layer canopy reflectance model.

nated/shadowed canopy and the ground (Li and Strahler 1986). In later studies, the opaque crowns in GO models were treated as a translucent turbid medium. Thus, GO and RT models were combined to obtain hybrid models, such as the GeoSAIL and 4SAIL2 models shown in Fig. 3. GO and hybrid models are developed primarily for forests (Huang *et al.* 2011a), but this concept can be applied to the modeling of row crop canopies (Yan *et al.* 2003; Zhao *et al.* 2010).

Using computer graphic techniques, computer simulation models firstly construct a very realistic scene of actual canopy, in which the radiative transfer take place. Then, computer simulation models compute the paths of photons inside the canopy using a Monte Carlo ray-tracking approach; i.e., photons from a specific direction are intercepted by canopy elements with a certain probability, where they are either absorbed or scattered into a new direction. Therefore, the reflectance and transmittance at a certain position with a specific view angle can be computed. Computer simulation models are considered to be computationally complex and difficult to invert (Schlerf and Atzberger 2006), but properly constructed computer simulation models are very accurate. Therefore they are usually used to validate RT models. For instance, Zhao *et al.* (2010) proposed a spectral directional reflectance model of row crops, and tested its performance by comparing with a 3-D computer simulation model by Qin and Gerstl (2000).

In practice, a model should be applied first to the predefined vegetation types that satisfy its hypotheses. In one study, several models might be used to fit different canopy layers (Eriksson *et al.* 2006), different vegetation types (Fang and Liang 2005), or even different crop growth stages (Yao *et al.* 2008), according to their respective geometric shapes. Second, researchers must trade off the acceptable accuracy level against computationally efficient models. For example, in current applications, the SAILH model is preferred for crops rather than the more accurate but more complex ACRM, as shown in Fig. 1.

4.2. Strategies for physical model inversion

Numerical solution techniques are necessary because of the complexity of physical models, where the commonly applied approaches include iterative optimization (OPT), lookup tables (LUTs), NNs, and SVR.

The OPT method (Fig. 4) first introduces a cost function between the observed (i.e., remotely sensed) and simulated canopy spectral reflectance. Next, the model input variables are adjusted repeatedly, including the LAI. The variables that minimize the cost function, i.e., those that yield the best match between the observed and simulated canopy reflectance, are selected as the inverted results (Jacquemoud *et al.* 1995). The LUT technique (Fig. 5) first constructs a LUT by running a forward canopy reflectance model. The LUT contains different combinations of input variables and the resulting canopy spectra. The values of the input variables in the LUT are generated randomly with uniform distributions, or vary by a specific step within a certain range (Atzberger and Richter 2012). Next, the observed canopy spectra are compared with the simulated spectra in the LUT one by one, and their fitness is measured by a cost function. The mean values of several sets of variable combinations that generate the best matches are taken as the inverted results. Statistical techniques can also be used to invert physical models. A synthetic training database similar to a LUT is first generated using physical models, and statistical techniques are then applied to determine the empirical relationships between the input variables and the simulated canopy spectrum in the database. Using these empirical relationships, the canopy variables can be computed from the observed canopy spectra. NNs (Trombetti *et al.* 2008; Duveiller *et al.* 2011), Bayesian expert systems (conditional probability networks) (Qu *et al.* 2008), and SVR (Durbha *et al.* 2007) have been tested for inverting physical models in previous studies, although the latter two approaches have not been applied widely.

OPT is the original approach for RT model inversion (Jacquemoud *et al.* 1995). Comparatively speaking, it yields fairly accurate results at the expense of computational efficiency because of the time-consuming process of optimization (Bacour *et al.* 2006). OPT is sensitive to the initial estimate of the solution, and it easily converges to a local minimum (Vohland *et al.* 2010). Previously, it was applied

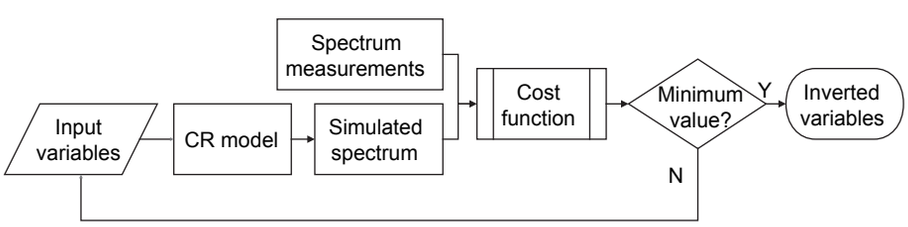

Fig. 4 Conceptual framework for iterative optimization (OPT) inversion. CR, canopy reflectance.

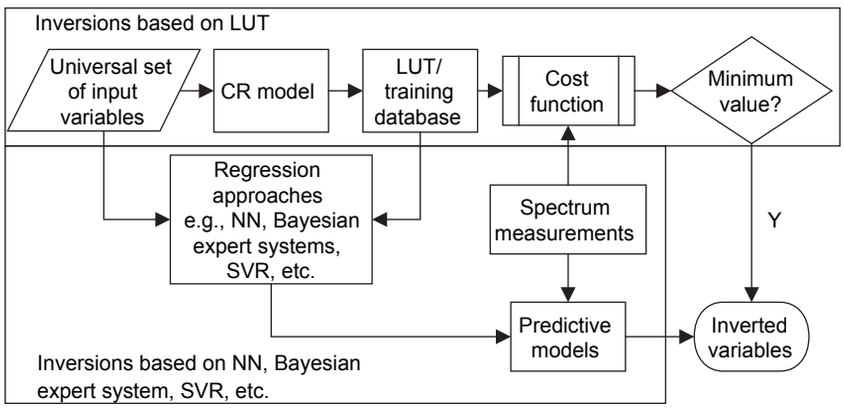

Fig. 5 Conceptual framework for inversion based on LUT, NN, Bayesian expert systems, or support vector regression (SVR). CR, canopy reflectance;

widely (Fig. 1), but it was not recommended in recent years. LUT and NN are considered to be accurate, fast, and simple inversion methods (Kimes *et al.* 2000; Weiss *et al.* 2002). In both the LUT and NN inversion strategies, the inversion accuracy depends on the size and accuracy of the LUT/ training database. Thus, it is necessary to consider the number of free parameters, their ranges, and probability distributions, as well as the desired inversion accuracy to determine the size of the LUT/training database. Weiss *et al.* (2000) proposed a LUT size of 100 000 as a compromise between inversion accuracy and computational efficiency when using the PROSAIL model with seven free variables. Based on the HyMap-retrieved spectrum of summer barley and the PROSAIL model, Vohland *et al.* (2010) argued that OPT is the most accurate inversion approach, followed by LUT and NN. However, there is little evidence to support the generality of this conclusion. Based on their inversion accuracy, computational efficiency, and comprehensive comparative complexity, both LUTs and NNs were recommended in previous studies (Weiss *et al.* 2000; Richter *et al.* 2009; Duan *et al.* 2014). At present, the LUT approach is dominant in terms of the number of applications (Fig. 1).

However, the inversion strategies employed at present are still hindered by the ill-posed problem (see section 4.3) and deviations between the simulated and remotely sensed spectrum. There are unavoidable errors in physical models, the *in situ* measurements, and the parameterization of some input variables; therefore, there is a bias between the simulated and remotely sensed spectra. These mismatches introduce errors into the retrived LAI values. Unfortunately, few relevant discussions have addressed these problems. In addition, appropriate approaches are required to find the best solutions of a LUT. At present, this problem is addressed by selecting the minimum value of a cost function or by multivariate regression (e.g., NN, Bayesian expert system, and SVR). However, the cost functions are far from perfect; meanwhile, few comparisons have been performed to determine the optimum regression method for LUT inversions in previous studies. In the future, better cost functions and more intelligent algorithms should be tested in inversions using LUTs, such as SVR and techniques of data mining.

4.3. The ill-posed problem

The inversion of canopy reflectance models is by nature an ill-posed problem; i.e., an underdetermined problem (Duan *et al.* 2014). There are always more unknown variables than independent spectral observations in physical models, and different sets of input variables may yield very similar synthetic reflectance results. This situation is further complicated by errors in both canopy reflectance models and *in situ* measurements (Durbha *et al.* 2007). The solutions to this ill-posed problem are summarized as follows.

First, the input variables used in physical models can be constrained based on prior knowledge. Prior knowledge refers to information that is known before a certain step in a process (Li *et al.* 1997). It is the basic prior knowledge to know the land use types and crop species in the target pixels, what enables us to assign well-adapted input variables separately to each crop (Dorigo *et al.* 2009; Verrelst *et al.* 2012). The expectations and/or ranges and probability distribution of crop variables can be applied to constrain the uncertainties in model parameterization by fixing insensitive parameters to their best guesses and constraining the ranges of free parameters (Combal *et al.* 2002; Si *et al.* 2012; Duan *et al.* 2014). Expectations of variables include the values of certain variables and the relationships that couple variables together, e.g., the water thickness and dry matter content can be coupled at a ratio of 4:1 (Darvishzadeh

et al. 2008; Vohland and Jarmer 2008). In addition, prior knowledge can be applied in cost functions in Bayesian LUT inversions (Li *et al.* 2001; Pinty *et al.* 2007).

Prior knowledge has been collected from the following sources in relevant studies: (1) contemporaneous remote sensing products (Houborg *et al.* 2007); (2) relevant studies and the experience of experts, e.g., phenological information (Si *et al.* 2012), best guesses of insensitive variables (Fang *et al.* 2003; Houborg *et al.* 2009), and variables that can be coupled together (Verhoef and Bach 2007; Darvishzadeh *et al.* 2008; Vohland and Jarmer 2008); (3) *in situ* measurements (Broge and Leblanc 2000); (4) model simulations (Wang *et al.* 2010); and (5) the results obtained during previous steps in the inversion process (Li *et al.* 1997).

Second, the dimensionality of the data can be increased by introducing uncorrelated multisource data. Essentially, the ill-posed problem occurs because the number of unknowns exceeds the number of equations. By increasing the dimensionality of the data, more known parameters and constraints can be introduced to help eliminate the uncertainties in physical models. In related studies, the multisource data employed to retrieved the LAI includes multitemporal data (Trombetti *et al.* 2008), multiangular data (Verrelst *et al.* 2012), and multiscale data (Fernandes *et al.* 2002).

Third, the strategies employed for physical model inversions can be improved. Innovative inversion strategies have been developed to reduce the uncertainties in physical model inversion, e.g., the multistage, sample-direction-dependent, target-decisions (MSDT) inversion strategy (Li *et al.* 1997), the Bayesian LUT inversion (Li *et al.* 2001; Pinty *et al.* 2007), and the object-based inversion (Atzberger 2004; Atzberger and Richter 2012; Laurent *et al.* 2014). Essentially, these strategies aim to constrain the uncertainties of variables by excavating, expressing and utilizing prior-knowledge from the aspects of variable optimization, multitemporal data and spatial signatures. For instance, the MSDT inversion technique requires the preferential inversion of the most sensitive parameter(s) using the bands that are most sensitive to it/them. The inverted results are then used to dynamically update the prior knowledge to retrieve other variables until all of the variables have been determined (Li *et al.* 1997). Such procedure significantly reduces the uncertainty of the variables step by step, and the inversion results can be refined gradually. These studies showed the feasibility of constraining the ill-posed problem by using innovative inversion strategies. However, model inversion still relies on operators' skill and is far from routinization at present, as Myneni *et al.* (1995) argued, "at the present time, inversion of physical models is more of an art than exact science". In the near future, inversion techniques that reduce the uncertainties in model inversions while retaining the universality of physical models will continue to be an interesting topic.

In conclusion, RT models are the most popular for crop canopies (Fig. 1), where the SAILH model provides an ideal compromise between accuracy and convenience. However, 3-D models provide more realistic simulations of canopies and the surrounding environment. In the future, given the development of high-spatial-resolution remote sensing, the data are more likely to comprise the pixels of pure canopies. Thus, more computationally efficient RT models can be applied, even for closed canopies of forests, as demonstrated by Zarco-Tejada *et al.* (2001). In addition, the need for large-scale studies demands more easily applied and easily inverted 3-D models that can be applied more easily, which represent more realistic scenes. In further studies of inversion strategies, the methods employed for physical model inversion should be improved dramatically to address the ill-posed problem and the differences between the simulated and measured spectra. More intelligent learning algorithms should be helpful for addressing the problems of LUTs.

4.4. The scale effects in crop LAI estimation

Notably, there are scale effects in crop LAI estimation. The cause of scale effect includes: the non-linearity of inversion models and the heterogeneity of land cover. The former is quite obvious; and the latter is illustrated as follows. The *in situ* measured LAI values and the spectra simulated with a CR model are at point scale, however, remotely sensed hyperspectral data are mainly (except *in situ* measurement of spectra) at pixel scale. Thus, there is an implicit assumption that the pixels applied in LAI retrieval are pure pixels. Such assumption is usually far from the reality, especially in China, where farmlands are usually composed of small parcels, resulting in mixed pixels. The existence of mixed pixels causes LAI estimations of different scales theoretically incomparable with each other, and also incomparable with *in situ* measurements. Studies of scale transformations are undertook to eliminate scale effects in LAI retrieval. Using hyperspectral data, Winter and Winter (1999) proposed the popular method of end-member detection referred as N-finder; Zortea and Plaza (2009) extracted end-members using the incorporation of spatial and spectral information. Fan *et al*. (2010a, 2012) proposed the equation of scale transformation based on the second derivative of the Kuusk model.

5. Hybrid inversion methods

The methods employed for LAI estimation based on sta-

tistical models perform well in small-scale studies when sufficient training samples are provided. These algorithms are simple and easy to implement. By contrast, methods based on physical models yield stable performance at a larger scale, thereby allowing us to analyze the factors that affect the canopy reflectance, but their algorithms are much more complex. Hybrid inversion methods aim to combine the advantages of both methods.

Two classes of hybrid inversions can be distinguished (Fig. 6). First, hybrid inversions at the physical model stage, i.e., simplifying the parameterization of physical models by introducing the characteristic parameters of input variables (Fang and Liang 2005), or improving the physical model itself based on empirical relationships (Fan *et al.* 2010b). Second, hybrid inversions at the inversion stage, i.e., constructing a statistical predictive model of LAI with a physical model. Two options are available. LAI values of some sample sites can be firstly estimated by inverting a physical model. Then, a statistical predictive model of LAI can be constructed using the estimated LAI values and the characteristic parameters computed from the remotely sensed canopies spectra. Otherwise, the statistical relationships can also be constructed between the characteristic parameters computed from synthetic spectra using a physical model, and the corresponding input LAI values for the physical model. The LAI values in the study area are then estimated using this statistical model (Eklundh *et al.* 2003; Houborg and Boegh 2008). For instance, Houborg and Boegh (2008) simulated the reflectance of barley using the ACRM model, then related LAI to normalized difference vegetation index (NDVI) and NIR spectral reflectance and related chlorophyll content to green spectral reflectance.

6. Selection of LAI retrieval approaches and prospects

In this review, we have explained the general concepts employed in LAI estimation based on remote sensing using hyperspectral data. We summarized the possible advantages and limitations of hyperspectral data in LAI estimation. The approaches used for LAI retrieval can be categorized into three types: approaches based on statistical models, physical models, and hybrid inversions. We highlighted the technical difficulties that may hinder LAI retrieval, e.g., the "curse of dimensionality" and the ill-posed problem, as well as their possible solutions. In this section, we compare three approaches for retrieving LAI (see section 6.1) and their possible development in future studies (see section 6.2).

6.1. Selection of LAI retrieval methods

First, the most important step of LAI retrieval is selecting an appropriate method according to the actual situation and the requirements of the study.

The scale of the study should be considered first. Statistical predictive LAI models are based simply on numerical relationships, and thus they rely greatly on the specific location, including the crop's condition and soil background reflectance. Therefore, statistical models are convenient for small-scale studies. By contrast, physical models are stable across a wide range of vegetation types and over a large area. Thus, LAI estimation by inverting physical models can be applied universally at a large scale.

Second, in terms of the data requirements, the ground truth LAI information is necessary to construct statistical predictive models. Thus, the accuracy of the ground truth

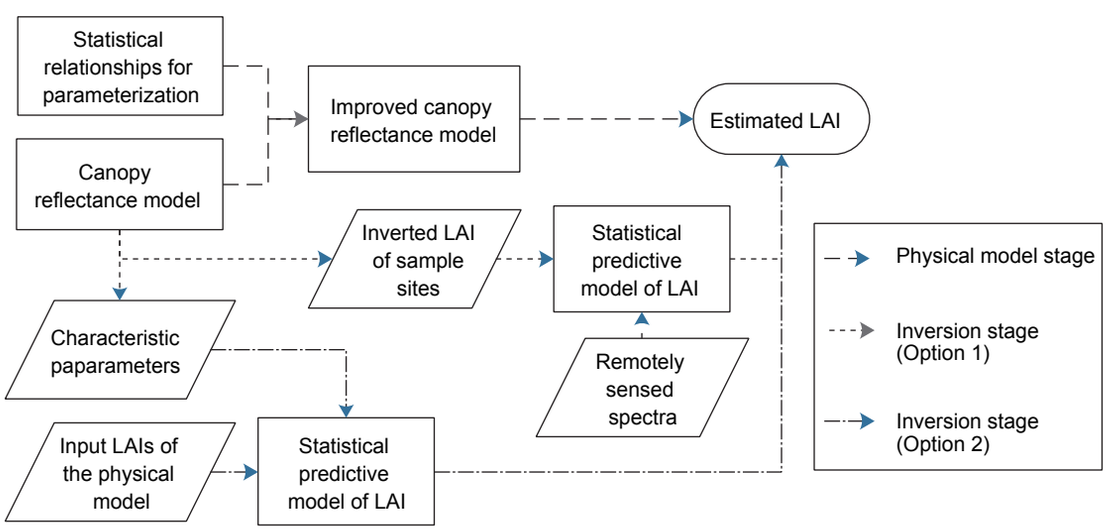

Fig. 6 Conceptual framework for hybrid inversion.

data determines the accuracy of LAI retrieval. In practice, physical models also need to be localized based on prior knowledge in order to ensure the correction of the input variables and to constrain the ill-posed problems (see section 5.3) (Jacquemoud *et al.* 1995). Nevertheless, physical models merely require general ranges and best guesses of parameters. The bias between the best guesses and the ground truth will not necessarily distort the inversion accuracy and the input variables can be optimized gradually during the inversion progress (Li *et al.* 1997). Thus, LAI estimation by inverting physical models is much less restricted with ground data. Some hybrid inversion strategies also allow the construction of statistical predictive models without *in situ* measurements of LAI (see section 5.4).

Third, in terms of the objective of the application, statistical predictive models are suitable for effective LAI monitoring (Yang *et al.* 2007a, b). Physical models can isolate and analyze the effects of each parameter and disturbance, which means that they can be used to study the influential factors and to estimate multiple vegetation variables simultaneously. More recent studies have aimed to improve physical models in terms of their clear theoretical basis, portability, and potential (Atzberger and Richter 2012; Verrelst *et al.* 2012).

In conclusion, this comparison shows that the two methods are complementary to some extent. A suitable approach for retrieving the LAI should be selected based on a comprehensive assessment of the actual situation and the requirements of the study. Statistical predictive models are preferred because of their simplicity and computational efficiency during dynamic monitoring or small scale applications, whereas LAI estimation methods based on physical models are selected mainly because of their portability, independence from the ground data, and ability to estimate multiple variables and to study the factors that influence the RT in canopies.

6.2. Prospects for future research

Based on our review, we propose a conceptual framework for LAI, as shown in Fig. 7, in which the general steps and key technical issues are outlined. In the context of LAI estimation using remote sensing techniques, our review provides adequate evidence to support the following prospects for future studies.

First, efforts should be made to utilize hyperspectral data effectively for LAI estimation. In section 2, we stated that

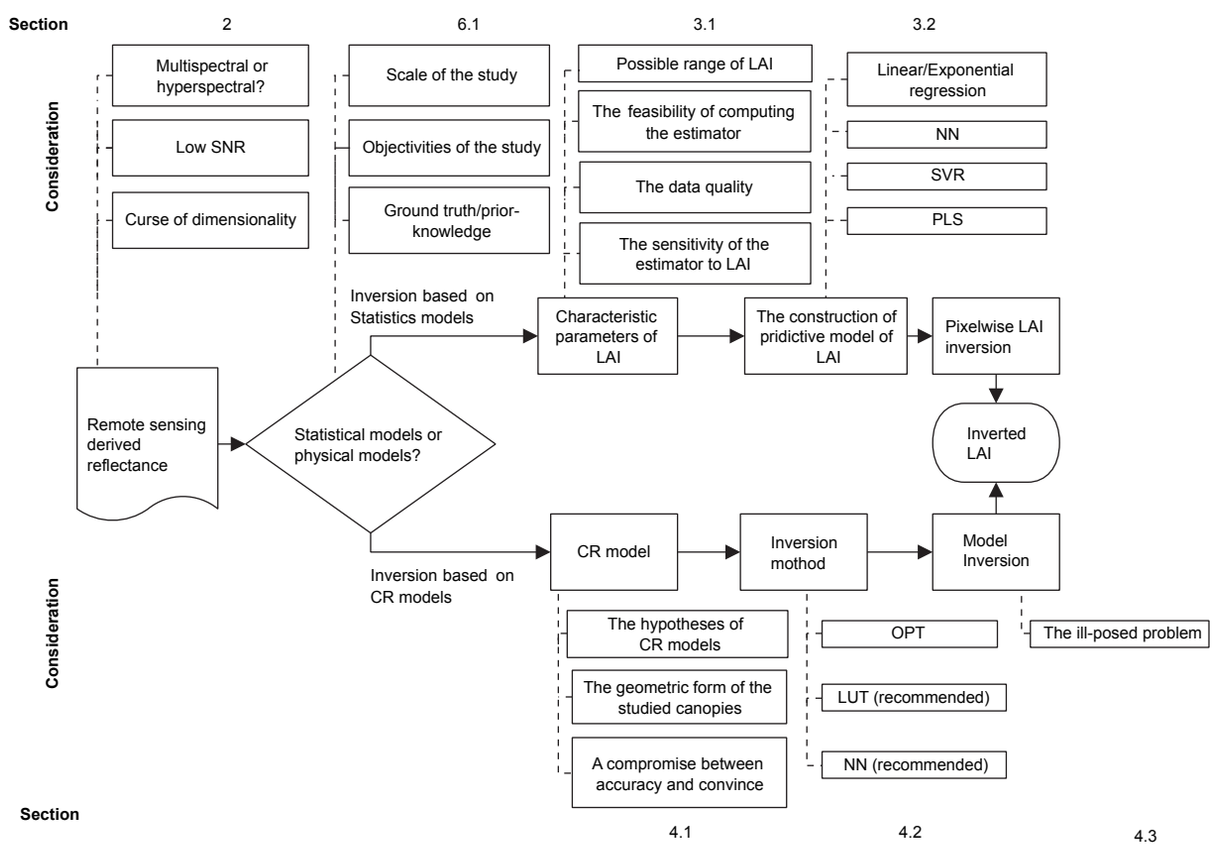

Fig. 7 A conceptual framework for LAI estimation. SNR, signal-to-noise ratio; PLS, partial least squares; LUT, look-up table.

even if hyperspectral data provide no direct improvements in LAI retrieval, they have the potential to reduce the uncertainties that affect LAI estimation by improving the estimated accuracy of other variables (e.g., chlorophyll/water content and average leaf angle) as well as improving atmospheric correction and pixel unmixing. Thus the accuracy and stabilities of LAI estimation can be improved indirectly using hyperspectral data. To achieve this objective, the input variables in physical models should be refined gradually during the inversion process, and the enhancement of other variables should contribute to LAI inversion. Therefore, the conventional inversion strategies for physical models are inadequate, and more sophisticated techniques should be developed. MSDT (Li *et al.* 1997), object-based inversion (Atzberger and Richter 2012), and Bayesian LUT inversion (Pinty *et al.* 2007) provide some innovative ideas, which warrant further investigation. Approaches that use hyperspectral data to eliminate disturbances from the atmosphere, soil background, and mixed pixels should also be studied further.

Second, multisource data, such as multisensor, multiangular, and multiscale data, as well as spatial information from remote sensing should be applied comprehensively in LAI estimations. The effects of the curse of dimensionality (see section 2.2) and the ill-posed problem (see section 5.3) on physical model inversions demand additional constraints, which can be obtained from multisource data. Previously, various types of multitemporal data (Dorigo *et al.* 2009), multiangular data (Verrelst *et al.* 2012), and multiscale data (Yan *et al.* 2003) have been tested, but spatial information has not been applied widely. In future studies, it would be useful to apply spatial information, including texture, spatial positions, and the topological relationships between intra- and interfeatures (objects), as demonstrated by Atzberger and Richter (2012), in LAI estimations and related processes, e.g., pixel unmixing. In addition, the further application of spatial information (e.g., object-based inversion) requires a fine spatial resolution, which must be obtained from remote sensing data of high spatial resolution. Another interesting objective would be to combine the advantages of hyperspectral and high-spatial-resolution data in LAI estimation.

Third, it is necessary to improve canopy reflectance models. Accurate canopy reflectance simulations are the basis of LAI estimation using physical models. However, the simulated canopy reflectance is sometimes far from realistic because of inaccurate parameterization and parameter optimization, especially in complex scenarios; e.g., row-planted crops. Moreover, in the current physical models, the different species present in canopies are distinguished using only input variables. These “universal” RT models for various species and various scenarios are beneficial for natural landscape studies, but they are not the optimum solution for agricultural studies. Various input variables cause difficulties during parameterization, as discussed above. Thus, in future studies, more accurate, specialized RT models should be studied intensively and developed for certain typical crop types and various scenarios to simplify the parameterization process, as well as improving the accuracy of the simulated canopy reflectance (Yan *et al.* 2003; Zhao *et al.* 2010).

Acknowledgements

This work is partially financed by the National High-Tech R&D Program of China (2012AA12A304) and the National Natural Science Foundation of China (41271112 and 41201089).

References

Atzberger C. 2004. Object-based retrieval of biophysical canopy variables using artificial neural nets and radiative transfer models. *Remote Sensing of Environment*, **93**, 53–67.

Atzberger C, Richter K. 2012. Spatially constrained inversion of radiative transfer models for improved LAI mapping from future Sentinel-2 imagery. *Remote Sensing of Environment*, **120**, 208–218.

Bacour C, Baret F, Béal D, Weiss M, Pavageau K. 2006. Neural network estimation of LAI, fAPAR, fCover and LAI×Cab, from top of canopy MERIS reflectance data: Principles and validation. *Remote Sensing of Environment*, **105**, 313–325.

Baret F, Clevers J, Steven M. 1995. The robustness of canopy gap fraction estimates from red and near-infrared reflectances: A comparison of approaches. *Remote Sensing of Environment*, **54**, 141–151.

Ben-Dor E, Patkin K, Banin A, Karnieli A. 2002. Mapping of several soil properties using DAIS-7915 hyperspectral scanner data — a case study over clayey soils in Israel. *International Journal of Remote Sensing*, **23**, 1043–1062.

Broge N H, Leblanc E. 2000. Comparing prediction power and stability of broadband and hyperspectral vegetation indices for estimation of green leaf area index and canopy chlorophyll density. *Remote Sensing of Environment*, **76**, 156–172.

Chen J M, Black T. 1992. Defining leaf area index for non-flat leaves. *Plant*, *Cell & Environment*, **15**, 421–429.

Chen J M, Cihlar J. 1996. Retrieving leaf area index of boreal conifer forests using Landsat TM images. *Remote Sensing of Environment*, **55**, 153–162.

Chen J M, Menges C H, Leblanc S G. 2005. Global mapping of foliage clumping index using multi-angular satellite data. *Remote Sensing of Environment*, **97**, 447–457.

Cohen W B, Maiersperger T K, Gower S T, Turner D P. 2003. An improved strategy for regression of biophysical variables and Landsat ETM+ data. *Remote Sensing of Environment*, **84**, 561–571.

Combal B, Baret F, Weiss M. 2002. Improving canopy variables estimation from remote sensing data by exploiting ancillary information. Case study on sugar beet canopies. *Agronomie*, **22**, 205–215.

Darvishzadeh R, Skidmore A, Schlerf M, Atzberger C. 2008. Inversion of a radiative transfer model for estimating vegetation LAI and chlorophyll in a heterogeneous grassland. *Remote Sensing of Environment*, **112**, 2592–2604.

Dorigo W, Richter R, Baret F, Bamler R, Wagner W. 2009. Enhanced automated canopy characterization from hyperspectral data by a novel two step radiative transfer model inversion approach. *Remote Sensing*, **1**, 1139–1170.

Duan S B, Li Z L, Wu H, Tang B H, Ma L, Zhao E, Li C. 2014. Inversion of the PROSAIL model to estimate leaf area index of maize, potato, and sunflower fields from unmanned aerial vehicle hyperspectral data. *International Journal of Applied Earth Observation and Geoinformation*, **26**, 12–20.

Durbha S S, King R L, Younan N H. 2007. Support vector machines regression for retrieval of leaf area index from multiangle imaging spectroradiometer. *Remote Sensing of Environment*, **107**, 348–361.

Duveiller G, Weiss M, Baret F, Defourny P. 2011. Retrieving wheat Green Area Index during the growing season from optical time series measurements based on neural network radiative transfer inversion. *Remote Sensing of Environment*, **115**, 887–896.

Eklundh L, Hall K, Eriksson H, Ardö J, Pilesjö P. 2003. Investigating the use of Landsat thematic mapper data for estimation of forest leaf area index in southern Sweden. *Canadian Journal of Remote Sensing*, **29**, 349–362.

Eklundh L, Harrie L, Kuusk A. 2001. Investigating relationships between Landsat ETM+ sensor data and leaf area index in a boreal conifer forest. *Remote Sensing of Environment*, **78**, 239–251.

Eriksson H M, Eklundh L, Kuusk A, Nilson T. 2006. Impact of understory vegetation on forest canopy reflectance and remotely sensed LAI estimates. *Remote Sensing of Environment*, **103**, 408–418.

Fang H, Liang S. 2005. A hybrid inversion method for mapping leaf area index from MODIS data: Experiments and application to broadleaf and needleleaf canopies. *Remote Sensing of Environment*, **94**, 405–424.

Fang H, Liang S, Hoogenboom G. 2011. Integration of MODIS LAI and vegetation index products with the CSM-CERES-Maize model for corn yield estimation. *International Journal of Remote Sensing*, **32**, 1039–1065.

Fang H, Liang S, Kuusk A. 2003. Retrieving leaf area index using a genetic algorithm with a canopy radiative transfer model. *Remote Sensing of Environment*, **8**5, 257–270.

Fan W J, Gai Y Y, Xu X R, Yan B Y. 2012. The spatial scaling effect of the discrete-canopy effective leaf area index retrieved by remote sensing. *Science China* (Earth Sciences), **43**, 280–286. (in Chinese)

Fan W J, Xu X R, Liu X C, Yan B Y, Cui Y K. 2010a. Accurate LAI retrieval method based on PROBA/CHRIS data. *Hydrology and Earth System Sciences*, **14**, 1499–1507.

Fan W J, Yan B, Xu X. 2010b. Crop area and leaf area index simultaneous retrieval based on spatial scaling transformation. *Science China Earth Sciences*, **53**, 1709–1716.

Feng R, Zhang Y, Yu W. 2013. Analysis of the relationship between the spectral characteristics of maize canopy and leaf area index under drought stress. *Acta Ecologica Sinica*, **33**, 301–307.

Fernandes R, Miller J R, Hu B, Rubinstein I G. 2002. A multi-scale approach to mapping effective Leaf Area Index in Boreal Picea mariana stands using high spatial resolution CASI imagery. *International Journal of Remote Sensing*, **23**, 3547–3568.

Filella I, Penuelas J. 1994. The red edge position and shape as indicators of plant chlorophyll content, biomass and hydric status. *International Journal of Remote Sensing*, **15**, 1459–1470.

Franke J, Roberts D A, Halligan K, Menz G. 2009. Hierarchical multiple endmember spectral mixture analysis (MESMA) of hyperspectral imagery for urban environments. *Remote Sensing of Environment*, **113**, 1712–1723.

Gao B C. 1993. An operational method for estimating signal to noise ratios from data acquired with imaging spectrometers. *Remote Sensing of Environment*, **43**, 23–33.

Gao B C, Montes M J, Davis C O, Goetz A F. 2009. Atmospheric correction algorithms for hyperspectral remote sensing data of land and ocean. *Remote Sensing of Environment*, **113**, S17-S24.

Garrigues S, Allard D, Baret F, Weiss M. 2006. Influence of landscape spatial heterogeneity on the non-linear estimation of leaf area index from moderate spatial resolution remote sensing data. *Remote Sensing of Environment*, **105**, 286–298.

Gastellu-Etchegorry J P, Martin E, Gascon F. 2004. DART: A 3D model for simulating satellite images and studying surface radiation budget. *International Journal of Remote Sensing*, **25**, 73–96.

Gonsamo A, Pellikka P. 2012. The sensitivity based estimation of leaf area index from spectral vegetation indices. *ISPRS Journal of Photogrammetry and Remote Sensing*, **70**, 15–25.

Guillen-Climent M L, Zarco-Tejada P J, Berni J A J, North P R J, Villalobos F J. 2012. Mapping radiation interception in row-structured orchards using 3D simulation and high-resolution airborne imagery acquired from a UAV. *Precision Agriculture*, **13**, 473–500.

Haboudane D. 2004. Hyperspectral vegetation indices and novel algorithms for predicting green LAI of crop canopies: Modeling and validation in the context of precision agriculture. *Remote Sensing of Environment*, **90**, 337–352.

Hernández-Clemente R, Navarro-Cerrillo R M, Zarco-Tejada P J. 2014. Deriving predictive relationships of carotenoid content at the canopy level in a conifer forest using hyperspectral imagery and model simulation. *IEEE Transactions on Geoscience and Remote Sensing*, **52**,

5206–5217.

Herrmann I, Pimstein A, Karnieli A, Cohen Y, Alchanatis V, Bonfil D J. 2011. LAI assessment of wheat and potato crops by VENμS and Sentinel-2 bands. *Remote Sensing of Environment*, **115**, 2141–2151.

Houborg R, Anderson M, Daughtry C. 2009. Utility of an image-based canopy reflectance modeling tool for remote estimation of LAI and leaf chlorophyll content at the field scale. *Remote Sensing of Environment*, **113**, 259–274.

Houborg R, Boegh E. 2008. Mapping leaf chlorophyll and leaf area index using inverse and forward canopy reflectance modeling and SPOT reflectance data. *Remote Sensing of Environment*, **112**, 186–202.

Houborg R, Soegaard H, Boegh E. 2007. Combining vegetation index and model inversion methods for the extraction of key vegetation biophysical parameters using Terra and Aqua MODIS reflectance data. *Remote Sensing of Environment*, **106**, 39–58.

Huang J, Zeng Y, Kuusk A, Wu B, Dong L, Mao K, Chen J. 2011a. Inverting a forest canopy reflectance model to retrieve the overstorey and understorey leaf area index for forest stands. *International Journal of Remote Sensing*, **32**, 7591–7611.

Huang J, Zeng Y, Wu W, Mao K, Xu J, Su W. 2011b. Estimation of overstory and understory leaf area index by combining hyperion and panchromatic QuickBird data using Neural Network method. *Sensor Letters*, **9**, 946–973.

Huemmrich K F. 2001. The GeoSail model: a simple addition to the SAIL model to describe discontinuous canopy reflectance. *Remote Sensing of Environment*, **75**, 423–431.

Jacquemoud S, Baret F, Andrieu B, Danson F, Jaggard K. 1995. Extraction of vegetation biophysical parameters by inversion of the PROSPECT+SAIL models on sugar beet canopy reflectance data. Application to TM and AVIRIS sensors. *Remote Sensing of Environment*, **52**, 163–172.

Jacquemoud S, Verhoef W, Baret F, Bacour C, Zarco-Tejada P J, Asner G P, François C, Ustin S L. 2009. PROSPECT+SAIL models: A review of use for vegetation characterization. *Remote Sensing of Environment*, **113**, S56–S66.

Jensen J R. 2009. *Remote Sensing of the Environment*: *An Earth Resource Perspective*. Pearson Education India, India.

Johnson L F, Billow C R. 1996. Spectrometry estimation of total nitrogen concentration in Douglas-fir foliage. *International Journal of Remote Sensing*, **17**, 489–500.

Kimes D, Knyazikhin Y, Privette J, Abuelgasim A, Gao F. 2000. Inversion methods for physically-based models. *Remote Sensing Reviews*, **18**, 381–439.

Kuusk A. 1991. The hotspot effect in plant canopy reflectance. In: *Photon-vegetation Interactions*: *Applications in Optical Remote Sensing and Plant Physiology*. Springer-Verlag, New York, USA.

Kuusk A. 1994. A multispectral canopy reflectance model. *Remote Sensing of Environment*, **50**, 75–82.

Kuusk A. 1995a. A fast, invertible canopy reflectance model. *Remote Sensing of Environment*, **51**, 342–350.

Kuusk A. 1995b. A Markov chain model of canopy reflectance. *Agricultural and Forest Meteorology*, **76**, 221–263.

Kuusk A. 2001. A two-layer canopy reflectance model. *Journal of Quantitative Spectroscopy and Radiative Transfer*, **71**, 1–9.

Laurent V C E, Schaepman M E, Verhoef W, Weyermann J, Chávez R O. 2014. Bayesian object-based estimation of LAI and chlorophyll from a simulated Sentinel-2 top-of-atmosphere radiance image. *Remote Sensing of Environment*, **140**, 318–329.

Lee K S, Cohen W B, Kennedy R E, Maiersperger T K, Gower S T. 2004. Hyperspectral versus multispectral data for estimating leaf area index in four different biomes. *Remote Sensing of Environment*, **91**, 508–520.

Li X, Gao F, Wang J, Strahler A. 2001. A priori knowledge accumulation and its application to linear BRDF model inversion. *Journal of Geophysical Research*, **106**, 11925–11935.

Li X, Gao F, Wang J, Zhu Q. 1997. Uncertainty and sensitivity matrix of parameters in inversion of physical BRDF model. *Journal of Remote Sensing*, **1**, 5–14. (in Chinese)

Li X, Strahler A H. 1986. Geometric-optical bidirectional reflectance modeling of a conifer forest canopy. *IEEE Transactions on Geoscience and Remote Sensing*, **6**, 906–919.

Li X H, Song X N, Leng P. 2011. A quantitative method for grassland LAI inversion based on CHIRS/PROBA data. *Remote Sensing for Land & Resources*, **3**, 60–66.

Lu D, Song K, Wang Z, Du J, Zeng L, Lei X. 2010. Application of wavelet transform on hyperspectral reflectance for soybean lai estimation in the songnen plain, China. In: *Proceedings of 2010 IEEE International Geoscience and Remote Sensing Symposium*. Honolulu, USA. pp. 2139–2142.

Myneni R B, Maggion S, Iaquinta J, Privette J L, Gobron N, Pinty B, Kimes D S, Verstraete M M, Williams D L. 1995. Optical remote sensing of vegetation: Modeling, caveats, and algorithms. *Remote Sensing of Environment*, **51**, 169–188.

Nilson T, Kuusk A. 1989. Reflectance model for the homogeneous plant canopy and its inversion. *Remote Sensing of Environment*, **27**, 157–167.

Othman H, Qian S E. 2006. Noise reduction of hyperspectral imagery using hybrid spatial-spectral derivative-domain wavelet shrinkage. *IEEE Transactions on Geoscience and Remote Sensing*, **44**, 397–408.

Perkins T, Adler-Golden S, Matthew M W, Berk A, Bernstein L S, Lee J, Fox M. 2012. Speed and accuracy improvements in FLAASH atmospheric correction of hyperspectral imagery. *Optical Engineering*, **51**, 1371–1379.

Pinty B, Lavergne T, Voßbeck M, Kaminski T, Aussedat O, Giering R, Gobron N, Taberner M, Verstraete M M, Widlowski J L. 2007. Retrieving surface parameters for climate models from Moderate Resolution Imaging Spectroradiometer (MODIS)-Multiangle Imaging Spectroradiometer (MISR) albedo products. *Journal of Geophysical Research* (Atmospheres (1984–2012)), **112**, 185–194.

Pu R, Gong P. 2004. Wavelet transform applied to EO-1 hyperspectral data for forest LAI and crown closure mapping. *Remote Sensing of Environment*, **91**, 212–224.

Pu R, Gong P, Biging G S, Larrieu M R. 2003. Extraction of red edge optical parameters from Hyperion data for estimation of forest leaf area index. *IEEE Transactions on Geoscience and Remote Sensing*, **41**, 916–921.

Pu R, Gong P, Yu Q. 2008. Comparative analysis of EO-1 ALI and hyperion, and landsat ETM+ Data for mapping forest crown closure and leaf area index. *Sensors*, **8**, 3744–3766.

Qin W, Gerstl S AW. 2000. 3-D scene modeling of semidesert vegetation cover and its radiation regime. *Remote Sensing of Environment*, **74**, 145–162.

Qu Y, Wang J, Wan H, Li X, Zhou G. 2008. A Bayesian network algorithm for retrieving the characterization of land surface vegetation. *Remote Sensing of Environment*, **112**, 613–622.

Richter K, Atzberger C, Vuolo F, Weihs P, D'Urso G. 2009. Experimental assessment of the Sentinel-2 band setting for RTM-based LAI retrieval of sugar beet and maize. *Canadian Journal of Remote Sensing*, **35**, 230–247.

Ross J. 1981. *The Radiation Regime and Architecture of Plant Stands*. Springer, New York, USA.

Saltelli A, Tarantola S, Chan K P S. 1999. A quantitative model-independent method for global sensitivity analysis of model output. *Technmetrics*, **41**, 39–56

Schlerf M, Atzberger C. 2006. Inversion of a forest reflectance model to estimate structural canopy variables from hyperspectral remote sensing data. *Remote Sensing of Environment*, **100**, 281–294.

Schlerf M, Atzberger C, Hill J. 2005. Remote sensing of forest biophysical variables using HyMap imaging spectrometer data. *Remote Sensing of Environment*, **95**, 177–194.

Si Y, Schlerf M, Zurita-Milla R, Skidmore A, Wang T. 2012. Mapping spatio-temporal variation of grassland quantity and quality using MERIS data and the PROSAIL model. *Remote Sensing of Environment*, **121**, 415–425.

Spanner M, Lee J, Miller J, McCreight R, Freemantle J, Runyon J, Gong P. 1994. Remote sensing of seasonal leaf area index across the Oregon transect. *Ecological Applications*, **4**, 258–271.

Tillack A, Clasen A, Kleinschmit B, Förster M. 2014. Estimation of the seasonal leaf area index in an alluvial forest using high-resolution satellite-based vegetation indices. *Remote Sensing of Environment*, **141**, 52–63.

Trombetti M, Riano D, Rubio M, Cheng Y, Ustin S. 2008. Multi-temporal vegetation canopy water content retrieval and interpretation using artificial neural networks for the continental USA. *Remote Sensing of Environment*, **112**, 203–215.

Verhoef W. 1984. Light scattering by leaf layers with application to canopy reflectance modeling: The SAIL model. *Remote Sensing of Environment*, **16**, 125–141.

Verhoef W, Bach H. 2007. Coupled soil-leaf-canopy and atmosphere radiative transfer modeling to simulate hyperspectral multi-angular surface reflectance and TOA radiance data. *Remote Sensing of Environment*, **109**, 166−182.

Verrelst J, Romijn E, Kooistra L. 2012. Mapping vegetation density in a heterogeneous river floodplain ecosystem using pointable CHRIS/PROBA data. *Remote Sensing*, **4**, 2866–2889.

Vohland M, Jarmer T. 2008. Estimating structural and biochemical parameters for grassland from spectroradiometer data by radiative transfer modelling (PROSPECT+SAIL). *International Journal of Remote Sensing*, **29**, 191–209.

Vohland M, Mader S, Dorigo W. 2010. Applying different inversion techniques to retrieve stand variables of summer barley with PROSPECT+SAIL. *International Journal of Applied Earth Observation and Geoinformation*, **12**, 71–80.

Wang D, Wang J, Liang S. 2010. Retrieving crop leaf area index by assimilation of MODIS data into a crop growth model. *Science China Earth Sciences*, **53**, 721–730.

Weiss M, Baret F, Leroy M, Hautecoeur O, Bacour C, Prevot L. 2002. Validation of neural net techniques to estimate canopy biophysical variables from remote sensing data. *Agronomie*, **22**, 547–553.

Weiss M, Baret F, Myneni R, Pragnère A, Knyazikhin Y. 2000. Investigation of a model inversion technique to estimate canopy biophysical variables from spectral and directional reflectance data. *Agronomie*, **20**, 3–22.

Widlowski J L, Taberner M, Pinty B, Bruniquel-Pinel V, Disney M, Fernandes R, Gastellu-Etchegorry J P, Gobron N, Kuusk A, Lavergne T, Leblanc S, Lewis P E, Martin E, Mõttus M, North P R J, Qin W, Robustelli M, Rochdi N, Ruiloba R, Soler C, *et al*. 2007. Third radiation transfer model intercomparison (RAMI) exercise: Documenting progress in canopy reflectance models. *Journal of Geophysical Research* (Atmospheres (1984–2012)), **112**, 139–155.

Winter E M, Winter M E. 1999. Autonomous hyperspectral endmember determination methods. In: *Proceedings of the International Society for Optical Engineering*, **3870**, Florence, Italy. pp. 150–158.

Wu W, Yang P, Meng C, Shibasaki R, Tang H, 2008. An integrated model to simulating sown area changes for major crops at a global scale. *Science in China* (Series D: Earth Sciences), **51**, 370–379.

Wu W B, Yang P, Tang H J, Zhou Q B, Shibasaki R. 2010. Characterizing spatial patterns of phenology in cropland of China based on remotely sensed data. *Agricultural Sciences in China*, **9**, 101–112.

Xia T, Wu W B, Zhou Q B, Zhou Y. 2013. Comparison of two inversion methods for winter wheat leaf area index based on hyperspectral remote sensing. *Transactions of the Chinese Society of Agricultural Engineering*, **29**, 139–147. (in Chinese)

Xiao Y, Zhao W, Zhou D, Gong H. 2013. Sensitivity analysis of vegetation reflectance to biochemical and biophysical variables at leaf, canopy, and regional scales. *IEEE Transactions on Geoscience and Remote Sensing*, **52**, 4014–4024.

Yan G, Jiang L, Wang J, Chen L, Li X. 2003. Thermal bidirectional gap probability model for row crop canopies

and validation. *Science in China* (Series D: Earth Sciences), **46**, 1241–1249.

Yang P, Shibasaki R, Wu W, Zhou Q, Chen Z, Zha Y, Shi Y, Tang H. 2007a. Evaluation of MODIS land cover and LAI products in cropland of North China Plain using in situ measurements and Landsat TM images. *IEEE Transactions on Geoscience and Remote Sensing*, **45**, 3087–3097.

Yang P, Wu W B, Tang H J, Zhou Q B, Zou J Q, Zhang L. 2007b. Mapping spatial and temporal variations of leaf area index for winter wheat in North China. *Agricultural Sciences in China*, **6**, 1437–1443.

Yang X, Huang J, Wu Y, Wang J, Wang P, Wang X, Huete A R. 2011. Estimating biophysical parameters of rice with remote sensing data using support vector machines. *Science China* (Life Sciences), **54**, 272–281.

Yao Y, Liu Q, Liu Q, Li X. 2008. LAI retrieval and uncertainty evaluations for typical row-planted crops at different growth stages. *Remote Sensing of Environment*, **112**, 94–106.

Zarco-tejada P J, Miller J R, Noland T L, Mohammed G H. 2001. Scaling-up and model inversion methods with narrowband optical indices for chlorophyll content estimation in closed forest canopies with hyperspectral data. *IEEE Transactions on Geoscience and Remote Sensing*, **39**, 1491–1507.

Zhao C J, Huang W J, Wang J H, Yang M H, Xue X Z. 2002. The red edge parameters of different wheat varieties under different fertilization and irrigation treatments. *Agricultural Sciences in China*, **1**, 745–751.

Zhao F, Gu X, Verhoef W, Wang Q, Yu T, Liu Q, Huang H, Qin W, Chen L, Zhao H. 2010. A spectral directional reflectance model of row crops. *Remote Sensing of Environmen*t, **114**, 265–285.

Zhu X H, Feng X M, Zhao Y S. 2011. Multi-scale MSDT inversion based on LAI spatial knowledge. *Science China* (Earth Sciences), **42**, 246–255. (in Chinese)

Zortea M, Plaza A. 2009. Spatial preprocessing for endmember extraction. *Geoscience and Remote Sensing*, *IEEE Transactions on Geoscience and Remote Sensing*, **47**, 2679–2693.

(Managing editor SUN Lu-juan)